LANGMUIR

Article

pubs.acs.org/Langmuir

Synthesis of Cone-Shaped Colloids from Rod-Like Silica Colloids with a Gradient in the Etching Rate

Fabian Hagemans,* Ernest B. van der Wee, Alfons van Blaaderen, and Arnout Imhof*

Soft Condensed Matter, Debye Institute for NanoMaterials Science, Utrecht University, Princetonplein 1, 3584 CC Utrecht, Netherlands

ABSTRACT: We present the synthesis of monodisperse cone-shaped silica colloids and their fluorescent labeling. Rod-like silica colloids prepared by ammonia-catalyzed hydrolysis and condensation of tetraethyl orthosilicate in water droplets containing polyvinylpyrrolidone cross-linked by citrate ions in pentanol were found to transform into cone-shaped particles upon mild etching by NaOH in water. The diameter and length of the resulting particles were determined by those of the initial rod-like silica colloids. The mechanism responsible for the cone-shape involves silica etching taking place with a varying rate along the length of the particle. Our experiments thus also lead to new insights into the variation of the local particle structure and composition. These are found to vary gradually along the length of the rod, as a result of the way the rod grows out of a water droplet that keeps itself attached to the flat end of the bullet-shaped particles. Subtle differences in composition and structure could also be resolved by high-resolution stimulated emission depletion confocal microscopy on fluorescently labeled particles. The incorporation of a fluorescent dye chemically attached to an amine-based silane coupling agent resulted in a distribution of fluorophores mainly on the outside of the rod-shaped particles. In contrast, incorporation of the silane coupling agent alone resulted in a homogeneous distribution. Additionally, we show that etching rods, where a silane coupling agent alone was incorporated and subsequently coupled to a fluorescent dye, resulted in fluorescent silica cones, the orientation of which can be discerned using super-resolution confocal microscopy.

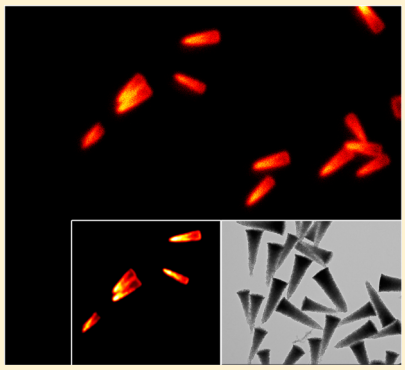

INTRODUCTION

Synthetic methodologies toward anisotropic colloidal particles have attracted increased attention over the past decade because of their great importance in nanomaterial assembly strategies. The interest in particles with less symmetric shapes comes from their potential in chemical, electronic, and optical applications.[1−3] Recent advances in the synthesis of anisotropic particles have supplied us with a large variety of anisotropic colloidal building blocks. Colloidal self-assembly of these anisotropic building blocks could lead to new functional materials with greater complexity than those currently available.[4−6]

Inorganic particles can be obtained in a large variety of shapes. In the literature, many methods are available to synthesize spherical and polyhedral particles from a large range of materials. Some examples are gold spheres,[7] silver polyhedra,[8] rhombohedral and cubic cadmium carbonate particles, and tetrahedral SnS microcrystals.[9] Rod- and board-like particles show special tunable optical properties upon self-assembling into colloidal liquid-crystalline phases but can also exhibit interesting catalytic properties.[10] These types of particles can be prepared from a large range of materials with varying sizes and aspect ratios. Some examples of these particles are goethite boards,[11,12] gold nanorods,[13] carbon nanotubes,[14] CdSe@CdS rods,[15] silicon nanowires,[16] and CdSe/Au[17] and CdSe/CsTe nanobarbells.[18]

These approaches are mostly limited to crystalline materials, but amorphous particles, such as silica, can be produced using a template-based synthesis. These shapes include cubes, peanuts, and ellipsoids.[19−21] These particles were synthesized by coating a hematite template with a layer of amorphous silica. These silica cubes have been observed to self-assemble in the presence of depletion attractions into a cubic or hexagonal lattice depending upon the depletant size. In the absence of attractive interactions, these particles were able to form hexagonal crystals with hollow site stacking. Silica, in particular, has the advantage that it can be easily chemically modified with various types of functional groups.[22] Recently, a new colloidal system of rod-like silica colloids was developed that does not require the use of a template that must be removed after the synthesis.[23,24] These particles can be produced in batch synthesis, have sufficiently low polydispersity to assemble into ordered phases, and can be easily functionalized by grafting or the incorporation of a silane coupling agent. This system allows for the quantitative real-space three-dimensional (3D) study of their self-assembly into various liquid crystalline phases.[25,26] The procedure starts with the synthesis of silica rods, as described by Kuijk et al.[23] These particles can be prepared in a simple one-pot synthesis by mixing ethanol, water, sodium citrate, ammonia, and tetraethyl orthosilicate (TEOS) with a solution of polyvinylpyrrolidone (PVP) in 1-pentanol. The rods grow from a water-rich droplet that serves as the locus for silica growth. Each rod grows from a

Received: February 22, 2016
Revised: March 24, 2016
Published: April 5, 2016

DOI: 10.1021/acs.langmuir.6b00678
Langmuir 2016, 32, 3970−3976

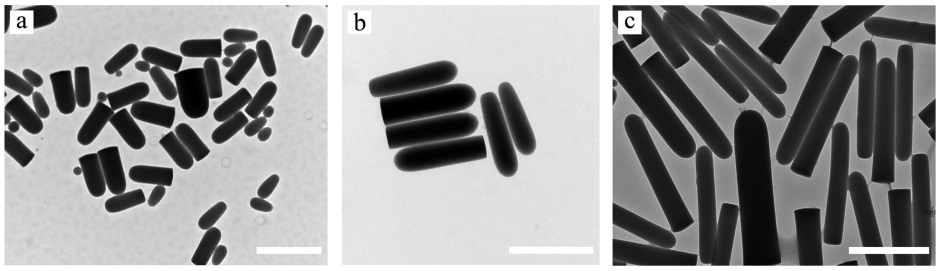

Figure 1. TEM images of typical monodisperse silica rods: (a) 1.60 ± 0.16 μm long rods, (b) 1.0 ± 0.2 μm long rods, and (c) 0.70 ± 0.06 μm long rods. Scale bars indicate 1 μm.

single water droplet containing PVP, in a pentanol phase (water-in-oil emulsion). In this emulsion droplet, which is stabilized by citrate ions, silica condensation takes place as a result of the presence of water, which is required for the hydrolysis of TEOS. As a result of the anisotropic supply of hydrolyzed TEOS, the particle predominantly grows from one side only. The particles have a bullet shape, with the round end having moved away from the water droplet during growth, while the flat end remained in contact with the aqueous phase until the end of the synthesis.

This mechanism has shown to be robust enough that it allows for modification of the shape and interactions of these silica rods. For example, it was shown that a hydrophobic segment could be added by the delayed addition of a hydrophobic silica precursor.[27] This yielded particles that consisted of hydrophilic and hydrophobic segments that self-assembled into micelle-like structures. A manganese oxide segment was introduced by *in situ* prepared nanoparticles that decorated the water droplet and resulted in self-propelling particles upon the addition of hydrogen peroxide.[28,29] A gold tip was introduced by the introduction of the Au(III)−PVP complex in the water droplet.[30] The shape of the particles could also be easily modified by changing the reaction conditions during particle growth.[31,32] The reaction temperature, ethanol concentration, and reagent addition time affected the diameter of the particle, allowing for the synthesis of segmented silica rods. The concentration of the base was shown to influence the locus of condensation of silicon alkoxide; at a high concentration of base, condensation took place predominantly at the droplet surface, leading to hollow silica rods.[30]

Kuijk et al.[33] noticed that the addition of a fluorescent dye that is incorporated after being chemically attached to the amine-functionalized end of a so-called silane coupling agent into the silica at the beginning of the reaction resulted in rods with a gradual decrease in fluorescence along their length. This was explained by a decreasing availability of the dye during growth, leading to a gradient in the dye concentration. It was shown that such a gradient in fluorescence can be used to determine the orientation of the rods even in concentrated systems.[25,26] On the contrary, the addition of the silane coupling agent 3-aminopropyltriethoxysilane (APTES) without a fluorescent dye chemically attached resulted in a homogeneous incorporation of amino groups throughout the particle. In addition, it is well-known that the base-catalyzed hydrolysis and condensation of silane coupling agents is slower than that of silicon tetraalkoxides in water alcohol mixtures.[34] Even without any dye present, reaction conditions are expected to change during particle growth, as silicon alkoxide and water are consumed and ethanol is formed. This may be expected to lead to a subtle chemical gradient as expressed in the level of condensation of the siloxane structure in the rods. Here, we confirm this by demonstrating that the silica produced early in the growth etches faster than the silica produced at the end of the reaction. Moreover, we make use of this chemical gradient to transform rods into cone-shaped particles. We further show that these particles can be made fluorescent, allowing them to be studied in real space. The fluorescent silica cones were imaged using two-dimensional (2D) continuous wave (CW)-gated stimulated emission depletion (STED) confocal microscopy. This technique allows for significant improvement of resolution in *xy*, where *z* is parallel to the optical axis, compared to conventional confocal microscopy, with a decrease in minimum separation of resolvable sources from ∼250 to <50 nm.[35−37] The particles can be prepared with high yield and maintenance of the original polydispersity, in a two-step synthesis.

■ EXPERIMENTAL SECTION

Experimental System. Silica rods with a length (L) of 1.60 ± 0.16 μm and a diameter (D) of 259 ± 64 nm (L/D = 6.1) were synthesized as described by Kuijk et al.[23] A typical transmission electron microscopy (TEM) image of these particles is shown in Figure 1a. In a 1 L glass laboratory bottle, 80.0 g of PVP (M_n = 40 kg/mol, Sigma-Aldrich) was dissolved in 800 mL of 1-pentanol (99%, ReagentPlus, Sigma-Aldrich). As soon as all PVP had been dissolved, 80.0 mL of ethanol (100%, Interchema), 22.7 mL of ultrapure water (Millipore system), and 5.3 mL of 0.18 M sodium citrate dihydrate (99%, Sigma-Aldrich) solution in water were added to the PVP−pentanol mixture. The content was homogenized by shaking the flask by hand. Subsequently, 18.0 mL of ammonia [25% (w/w) in water, Sigma-Aldrich] and 6.7 mL of TEOS (98%, Sigma-Aldrich) were added. After mixing the content, the bottle was left to rest for 24 h. The length of these rods can be easily chosen from 300 nm to 3 μm by increasing or decreasing the concentration of ammonia, PVP, water, or ethanol.[23] The aspect ratio of the silica rods was varied by increasing the amount of ammonia to 19 mL for 1.0 ± 0.2 μm rods (L/D = 3.5) and 20 mL for 0.70 ± 0.06 μm rods (L/D = 2.5). TEM images of the initial silica rods are shown in panels b and c of Figure 1.

APTES-functionalized silica rods (L/D = 4, and L = 0.90 ± 0.02 μm) were prepared using 18 mL of ammonia, and together with the precursor TEOS, 155 μL of APTES (98%, Sigma-Aldrich) was added.

Silica rods with a gradient in fluorescence were prepared using a similar recipe. First, 27 mg of fluorescein isothiocyanate isomer I [FITC, Sigma-Aldrich, ≥90%, high-performance liquid chromatography (HPLC) grade] was dissolved in 5 mL of absolute ethanol (Sigma-Aldrich), and subsequently, 35.0 μL of APTES (98%, Sigma-Aldrich) was added. This solution was stirred for 3 h in the dark. Second, 18.0 g of PVP (M_n = 40 kg/mol, Sigma-Aldrich) was dissolved in 160 mL of 1-pentanol (99%, ReagentPlus, Sigma-Aldrich). As soon as all PVP had been dissolved, 13 mL of ethanol (100%, Interchema), 5.0 mL of the APTES−dye solution, 5.1 mL of ultrapure water (Millipore system), and 1.2 mL of 0.18 M sodium citrate dihydrate (99%, Sigma-Aldrich) solution in water were added to the PVP−pentanol mixture. The content was homogenized by shaking the flask

DOI: 10.1021/acs.langmuir.6b00678
Langmuir 2016, 32, 3970−3976

by hand. Subsequently, 4.1 mL of ammonia [25% (w/w) in water, Sigma-Aldrich] and 1.5 mL of TEOS (98%, Sigma-Aldrich) were added. After mixing the content, the bottle was left to rest for 24 h.

The particles were transferred to ethanol by centrifugation (1500*g* for 1 h) and redispersed in ethanol (96%, Interchema). Subsequently, the particles were washed with ethanol, water, and 2 times with ethanol by centrifugation (1500*g* for 15 min) and redispersion steps. To improve the monodispersity, small rods were removed by multiple centrifugation (700*g* for 15 min) and redispersion steps and large rods were removed by centrifugation at 200*g* for 5 min and removing the sediment.

A small part of the APTES-functionalized rods (0.22 mL, 10 g L^{-1}) was fluorescently labeled with FITC for visualization with (2D STED) confocal microscopy by adding 2.0 mg of FITC (≥90%, HPLC grade, Sigma-Aldrich). The reaction mixture was stirred slowly for 24 h. Next, the particles were washed with ethanol (100%, Interchema) 4 times.

Etching of Silica Rods. Silica rods were etched as follows. In a 40 mL glass laboratory bottle, 1.15 mL of 21 g L^{-1} silica rods in ethanol was transferred into 40.0 mL of 3 mM NaOH (tablets, Sigma-Aldrich) solution in water. The bottle was left to rest for 24 h. Next, the particles were washed with ethanol (100%, Interchema) 3 times.

The etched APTES-functionalized rods were fluorescently labeled with FITC for visualization with 2D CW-gated STED confocal microscopy by adding 8 mg of FITC (Sigma-Aldrich). The reaction mixture was stirred slowly for 24 h. Next, the particles were washed with ethanol (100%, Interchema) 4 times.

Particle Characterization. Two-dimensional STED confocal microscopy images were taken using a Leica TCS SP8 equipped with a CW depletion laser and a 100×/1.4 confocal oil immersion objective. STED was performed using a solid-state laser at a wavelength of 592 nm, and imaging in gated STED mode was performed using an excitation of fluorescein at 488 nm with a white light continuum laser. The images were taken at a resolution of 1024 × 1024 pixels. The particles were index-matched in a mixture of 85% (w/w) glycerol (≥99%, Sigma-Aldrich) and 15% (w/w) ultrapure water (n_D^{20} = 1.4515). TEM images were taken using a Philips Tecnai 12 electron microscope. The width, length, and cone angle of the particles were determined by measuring between 100 and 150 particles by hand using the TEM imaging platform iTEM (version 5.0, Soft Imaging System GmbH). The width, length, and cone angle of the particles are displayed as a length/width/cone angle ± polydispersity. The polydispersity represents the width of the size distribution.

■ RESULTS AND DISCUSSION

Compositional and Structural Differences. A fluorescent dye coupled to a silane coupling agent (APTES) was added at the start of the particle growth. This resulted in a gradient of decreasing fluorescence along the length during the growth of the particle, as observed previously (Figure 2a).[33] However, closer inspection of the fluorescence pattern using a form of super-resolution microscopy, 2D CW-gated STED confocal microscopy[35−37] (Figure 2a), showed the fluorescence to be mainly concentrated in a thin outer layer. This layer could previously not be distinguished using standard confocal microscopy.[33] This therefore led us to the conclusion that the fluorescent dye−silane coupling agent reacts to the growing rods mainly from the oil phase, as opposed to from within the water droplet. The reaction product of the dye and silane coupling agent seems not to dissolve well enough in the emulsion droplet to form a homogeneous distribution of fluorescence throughout the particle, instead, forming a thin fluorescent layer on the outside of the particles. The gradient of fluorescence along the length of the particles indicates that, as the rods grow, there is a decrease in the dye incorporation in the outer silica layer. This also indicates that it is likely that some TEOS also reacts directly from the oil phase, instead of

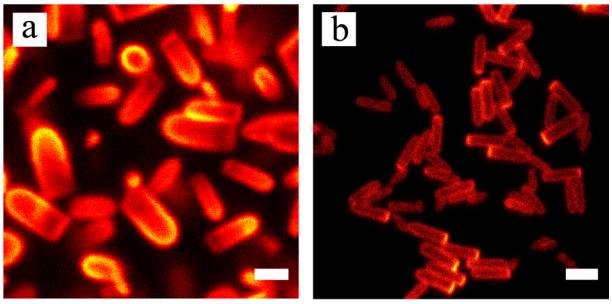

Figure 2. Two-dimensional STED confocal microscopy images of (a) FITC−APTES-functionalized silica rods showing a gradient in the dye concentration along their length and a step in the dye concentration along their width and (b) APTES-functionalized silica rods, post-modified with FITC, showing a constant dye concentration along their length, except for their flat end, and a step in the dye concentration along their width. Scale bars indicate 1 μm.

from the water droplet, and that also this reactant might be depleted toward the end of the rod growth.

However, an interesting phenomenon is observed upon the incorporation of the silane coupling agent alone, without a dye attached, and subsequently attaching the dye after rod synthesis (Figure 2b). Close inspection, again using 2D STED confocal microscopy, showed an entirely different fluorescence distribution along the length of the particle (Figure 2b). Here, the fluorescence was constant throughout the entire length of the particle, except for at the flat end, where the fluorescence intensity was greater. This demonstrates a constant distribution of APTES throughout the whole particle, unlike the gradient that we observed previously for the case of the FITC−APTES incorporation. Our knowledge of the particle growth mechanism is consistent with this observation: as a result of the non-zero solubility of water and the ammonia base in the oil phase, APTES can technically grow (undergo a condensation reaction and, thus, attach to the rod) from both the continuous oil phase and the emulsion droplet interior. However, because the amine functionality is more soluble in the water droplet, it would be expected that growth should predominantly occur from there. The increased fluorescence at the surface of the particle can be explained as a result of another reason. The structure of the particle is insufficiently porous to allow for the FITC molecules to diffuse in, and therefore, the dye mainly reacts with groups present at the surface of the particle. This nonhomogenous fluorescence pattern was not observed with conventional confocal microscopy, as described by Kuijk et al.,[33] because of the significantly higher resolution of STED confocal microscopy. These results show us that the chemical composition changes with the solubility of the reactant in each phase and the availability of monomer and/or the availability of TEOS, which is known to be important for the incorporation of the coupling agent inside a growing particle.[34] Because, during the reaction, the reactants APTES, when it is used, and TEOS are consumed and ethanol is produced, it is likely that a subtle gradient is present in the particle.

Etching. To modify the shape of silica rods, several non-functionalized, undyed rods (around 1.0 μm long) were etched for 24 h in a NaOH solution in water at varying concentrations of the etchant. A typical TEM image of these particles is shown in Figure 1. Using concentrations of 3 mM NaOH and 0.6 g L^{-1} particles, we were able to prepare monodisperse cone-shaped colloids with varying aspect ratios and cone angles.

DOI: 10.1021/acs.langmuir.6b00678
Langmuir 2016, 32, 3970−3976

These particles had an average length of 804 ± 124 nm (polydispersity) and an average angle at the tip of 17° ± 4° (polydispersity), where the length was found to slightly decrease upon etching. The surface of the particles had become rougher because of the etching process. The flat ends of the particles had also become slightly rougher, indicating a slight yet less severe etch compared to the round tips, where the rod has started to grow. A typical TEM image of these particles is shown in Figure 3a. The length of the etched particles was determined by the length of the original rod used for the synthesis. The wide range of aspect ratios that we can obtain from the synthesis of rods gives us the possibility to obtain a wide variety of cone-shaped particles with tunable length and angle.

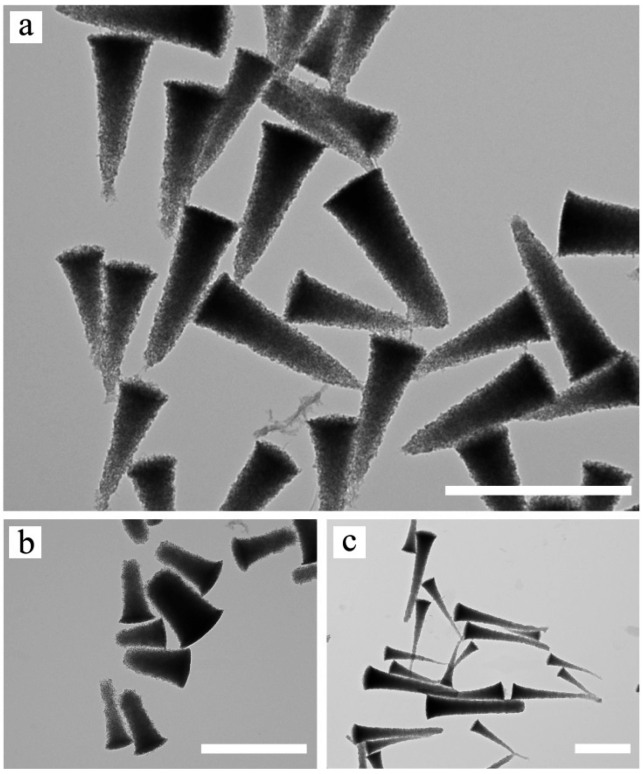

Figure 3. Cone-shaped silica colloids with varying length (L) by etching silica rods at 3 mM NaOH for 24 h: (a) L = 804 ± 124 nm (polydispersity), (b) L = 604 ± 60 nm, and (c) L = 1350 ± 379 nm. Scale bars indicate 1 μm.

In panels b and c of Figure 3, we show TEM images of cone-shaped particles with smaller and larger lengths, respectively. These particles had an average length of 604 ± 60 nm and an angle of 15° ± 4.5° (for the short rods) and an average length of 1350 ± 379 nm and angle of 10° ± 2.5°(for the long rods). The short rods did not contain a sharp tip: the gradient in etching rates was not steep enough to cause a clear difference in etching rates between each end. It can also be observed that the long cones have a slightly bent tip: the tip became thin and flexible, and this is presumably due to bending during drying.

The concentration of sodium hydroxide used in the etching process strongly influences the final morphology of the particle. At low concentrations (0.5 mM NaOH), the final particle shapes are affected differently than at higher concentrations (panel a versus panel d of Figure 4). At low concentrations, the flat end of the particle showed clear signs of tapering but the rounded end appears to be almost untouched, resulting in a concave overall shape. More interestingly, the middle section of the particle is also surrounded by a thin cylindrical shell that was not observed in the final shapes of high etchant concentrations (Figure 3 compared to Figure 4d).

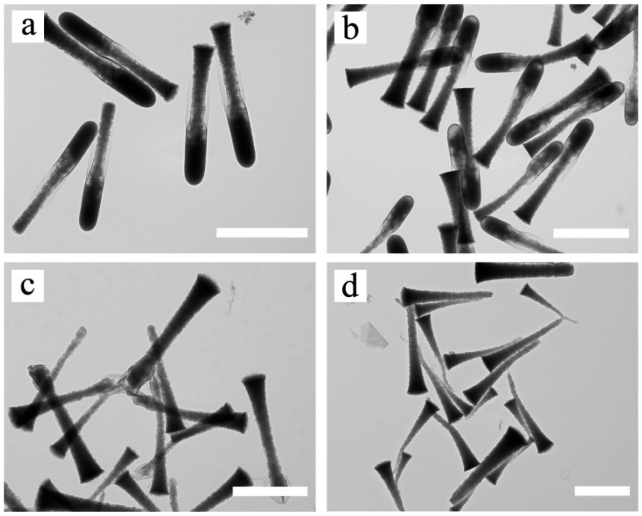

Figure 4. Silica colloids with varying shapes formed by etching silica rods for 24 h at different NaOH concentrations: (a) 0.5 mM, (b) 1 mM, (c) 2 mM, and (d) 3 mM. Scale bars indicate 1 μm.

At higher concentrations (1 mM NaOH; Figure 4b), the result was comparable. However, one now observes a change at the round side of the particle; it appears to be a more open (porous-like) structure, which is again surrounded by a dense and thin cylindrical silica shell. The shell around the tip appears to be thicker than the shell present around the middle when using 0.5 mM NaOH. This dense shell was less soluble than the inner part of the tip of the silica rod. The base increased the porosity of the shell and subsequently etched the apparently faster etchable inner parts of the rod.

Increasing the concentration to 2 mM NaOH (Figure 4c) resulted in cone-shaped particles where the rounded side of the particles ended up being surrounded by a thin shell of silica. Here, the rounded end caught up with the etching of the flat end of the particle: the rounded side of the particle was much more soluble but also less accessible than the flat side of the particle. At higher concentrations (3 mM NaOH; Figure 4d), the thin silica shell completely disappeared: the particle transformed into a cone shape. It must be noted that the particle shapes after 24 h are the final shapes: no further etching took place because the base was neutralized sufficiently by reacting with the weakly acidic silanol groups that resulted from dissolving silica. This lowering of the pH with time also makes it clear that final particle morphologies do depend upon not only the NaOH concentrations used but also the amount of silica being etched.

From the different degrees of etching along the length of the particle, we conclude that there must be a gradient in chemical composition throughout the particle. Because a surface with a perfectly homogeneous chemical composition would have a constant etching rate along the surface, no corrugation should appear over time. In the case of a surface with a varying composition and, therefore, also varying etching rate, a roughening of the surface could result. However, if the composition and etching rates varied along the surface with a smooth gradient, one would expect the surface to remain flat

DOI: 10.1021/acs.langmuir.6b00678
Langmuir 2016, 32, 3970−3976

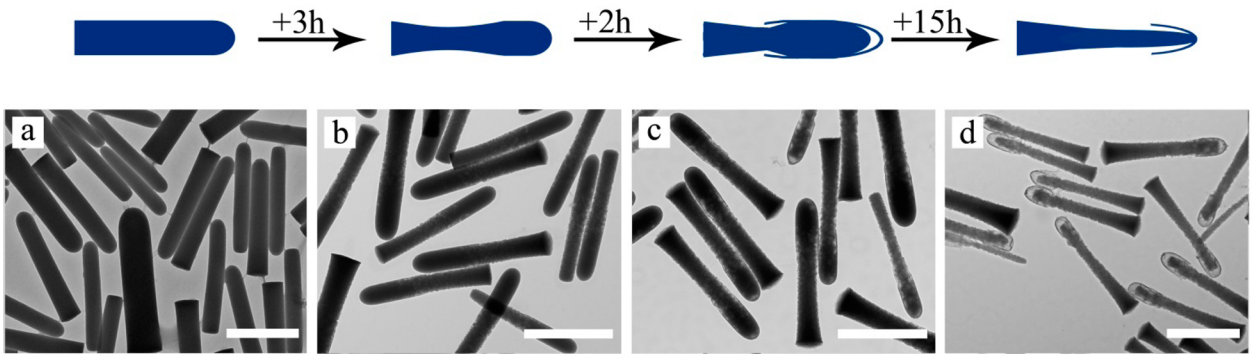

Figure 5. Time-dependent transformation of silica rods at a concentration of 3 mM NaOH: (a) initial rods, (b) 3 h, (c) 5 h, and (d) 20 h. Scale bars indicate 1 μm.

but become tilted with respect to its original position. To observe a gradient in etching rate, we took TEM images of the sample during etching. Figure 5 shows the time-dependent transition of the particles from a rod to a cone-shaped particle and its intermediate states at a concentration of 3 mM NaOH. At short times, predominantly the second half of the bullet nearer to the flat end is etched, whereas the first half of the particle seems untouched. However, at longer times (5 h), the inner side of the rod partly dissolves away, leaving behind a thin shell around the particle. Finally, after 20 h, a cone-shaped particle with a thin silica shell is found. Thus, indeed there exists a gradient in the etching rate along the silica rods, but the presence of an outer thin, likely more condensed, silica shell complicates the mechanism.

The growth mechanism that we propose is as follows: during the synthesis of the rod-like silica particles, two processes are occurring simultaneously. The first process is the growth of the rod from the emulsion droplet. Hydrolyzed TEOS is mainly supplied from within the droplet; this causes the particle to grow in one direction only: out of the droplet in the form of a rod with a PVP–water droplet attached on its flat end. This growth is the fastest at the start of the reaction when hydrolyzed TEOS is in the highest abundance. It is known that, in base-catalyzed hydrolysis–condensation reactions of silicon tetraalkoxides, the condensation reactions are faster than that of hydrolysis.[38] In the case of Stöber growth of silica spheres, the resulting silica is by far not fully condensed: our previous work using quantitative silicon nuclear magnetic resonance (NMR) has shown this to be the case for the rod growth as well.[33] However, as TEOS is consumed, also the condensation reactions slow. This most likely results in more fully condensed silica.

From the literature, it is well-known that fast condensation of silicon alkoxide will result in porous structures, whereas slow condensation will result in denser silica.[39,40] This is caused by the formation of oligomers in the water phase at high TEOS concentrations, which aggregate less densely than condensing monomer units. We hypothesize that this kinetically induced difference in the condensation level causes the gradient in composition along the length of the rod. A similar inhomogeneity has been found in the silica layers deposited with the Stöber process around gold particles and pure Stöber spheres, which resulted in yolk–shell particles after etching.[41]

The second process taking place during rod growth is the hydrolysis and condensation of TEOS from the pentanol phase on the freshly grown rod. During the reaction, a small amount of hydrolyzed TEOS will be present in the pentanol phase. These monomers can either diffuse to the water droplet or condense on the freshly grown rod directly. This process is slow because of the low concentration of hydrolyzed TEOS in the pentanol phase, which is, in turn, caused by the lower concentration of water and ammonia in the pentanol phase, both of which are required for the hydrolysis of TEOS. This slow process causes the formation of a thin but most likely more dense silica shell around the rod. Figure 4b shows etched particles, where this thin shell can be easily seen. The existence of this shell has recently been inferred in a publication by Longbottom et al.[29] Similarly, a dye–silane coupling agent shell can be seen in dyed, unetched particles using super-resolution confocal microscopy (Figure 2a).

The gradient in composition along the length of the rod caused a difference in the dissolution rate in the same direction: the part of the rod with the rounded side etches faster than the part with the flat end, which is more condensed. However, the thin silica shell, which is more prominent around the "older" rounded half of the rod, having been exposed longer to the growth solution, temporarily protects this half of the rod from dissolution. Transport of materials to and from the inner core through this thin shell is necessarily slowed. Therefore, dissolution is delayed at the rounded side of the particles and gives rise to the observed intermediate states. As soon as the solution becomes saturated with silicate ions and the pH decreases by action of the resulting silanol groups, the etching stops and the morphology of the particles will change no further.[39]

Fluorescent Silica Cones. Real-space analysis of the phase behavior of silica cones requires the particles to be fluorescently labeled. For silica rods, three methods were previously explored by Kuijk et al.[33] Because growing a thick layer of fluorescent silica around a silica cone will result in the loss of the shape, we need a method that labels the cores of the particle. However, etching silica rods with a gradient in fluorescence resulted in the loss of fluorescence. During etching, the outer layer etched away precisely the part that contained the highest concentration of dye. To prepare fluorescent silica cones, we instead etched 0.9 μm APTES-functionalized silica rods, where the silane coupling agent was added at the start of the rod synthesis, in 5 mM NaOH solution. The average size of these particles was determined using TEM; the particles had a length of 887 ± 121 nm, a width of 275 ± 60 nm (L/D = 3.2), and a tip angle of 12.5° ± 1.9°. Earlier, we proposed that the amine functionality was spread throughout the particle. If this were the case, it would allow us to create a FITC-labeled silica cone. Upon labeling the particle with FITC, we indeed find a fluorescence

DOI: 10.1021/acs.langmuir.6b00678
Langmuir 2016, 32, 3970–3976

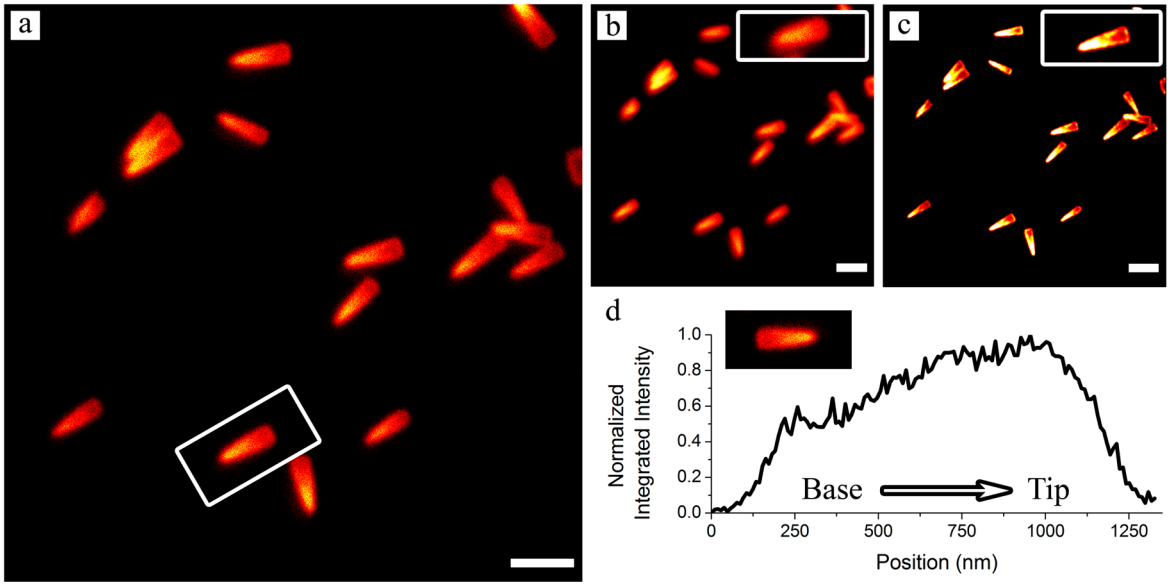

Figure 6. Fluorescent cone-shaped particles imaged using (a) 2D STED confocal microscopy, (b) confocal microscopy, (c) panel a deconvoluted using Huygens Professional software, and (d) normalized integrated intensity from the highlighted particle in panel a along its length after projection of the dye intensities taken at different heights into one 2D image. The normalized integrated intensity increases from the base of the particle to the tip. Scale bars indicate 1 μm.

signal from the particles. However, the top layer, which coupled to FITC earlier, has been etched away. These particles were imaged using 2D STED confocal microscopy as described in the Experimental Section. Figure 6a shows that the fluorescence is again mainly present at the surface of the particle if the silane coupling agent is added at the beginning of the synthesis. This indicates that the functional groups are present throughout the particle but that groups lying deeper in the particle are not reached by the fluorescent dye. A core−shell structure was observed for the APTES-functionalized initial silica rods, which can also be observed for the silica cones. However, the tip of the particle seems to be more fluorescent than the tail of the particle; this type of profile was not observed for the initial silica rods. This gradient in fluorescence is probably caused by a gradient in porosity formed during the etching process. As a result of the increased porosity at the tip, the dye can diffuse further into the particle and, thus, react with the already present amine functionalities. At the base, the porosity is less increased; here, the fluorescence is clearly weaker. We confirm this by integrating the intensity of a z projection of the particle line by line. Figure 6d shows that the normalized integrated intensity gradually increases from the base of the particle to the sharp tip, and thus, the concentration of amine functionalities coupled to FITC also gradually increases with the length of the particle. Using standard confocal microscopy (Figure 6b), we could not observe the pattern of fluorescence shown in Figure 6a because of the significantly lower resolution. Furthermore, the flat end of the particle could hardly be distinguished from the tip. After deconvolution of the 2D STED confocal microscopy image using the software package Huygens Professional 5.5 Scientific Volume Imaging resulting in Figure 6c, we can observe the orientation of the particle quite well.[42] The core−shell structure becomes clearer in these images, and the increased intensity at the tip is still present.

■ CONCLUSION

We presented a new method to prepare anisotropic colloidal particles with tunable length and shape by etching bullet-shaped silica rods. The particles obtained have similar polydispersity to the initial bullet-shaped rods, can be prepared in batch synthesis, and are tunable in length. By exploiting the NaOH concentration and reaction time, we synthesized silica structures with interesting intermediate shapes, such as cones and concave rods. The method makes use of our finding that the chemical composition of silica rods contains a gradient, which results from their growth mechanism. We further demonstrated that these particles can be prepared with a homogeneous distribution of amine functional groups, which allows for the fluorescent labeling of these particles. These particles can be imaged using STED confocal microscopy, which allows for the real-space study of the phase behavior of these particles. We anticipate that controlling composition gradients in particles opens further opportunities for the development of rod-like silica particles with additional functionalities.

■ AUTHOR INFORMATION

Corresponding Authors

*E-mail: f.hagemans@uu.nl.
*E-mail: a.imhof@uu.nl.

Notes

The authors declare no competing financial interest.

■ ACKNOWLEDGMENTS

This research is funded by the Netherlands Organisation for Scientific Research (NWO). Alfons van Blaaderen and Ernest B. van der Wee acknowledge the European Research Council (ERC) under the European Union's Seventh Framework Programme (FP/2007-2013)/ERC Grant Agreement 291667.

DOI: 10.1021/acs.langmuir.6b00678
Langmuir 2016, 32, 3970−3976

■ ABBREVIATIONS USED

TEOS, tetraethyl orthosilicate; PVP, polyvinylpyrrolidone; APTES, 3-aminopropyltriethoxysilane; 2D CW-gated STED confocal microscopy, two-dimensional continuous-wave-gated stimulated emission depletion confocal microscopy; TEM, transmission electron microscopy; FITC, fluorescein isothiocyanate

■ REFERENCES

(1) Glotzer, S. C.; Solomon, M. J. Anisotropy of building blocks and their assembly into complex structures. *Nat. Mater.* **2007**, *6*, 557−562.

(2) Yang, S. -M; Kim, S. -H; Lim, J. -M; Yi, G. -R Synthesis and assembly of structured colloidal particles. *J. Mater. Chem.* **2008**, *18*, 2177−2190.

(3) Perro, A.; Reculusa, S.; Ravaine, S.; Bourgeat-Lami, E.; Duguet, E. Design and synthesis of Janus micro- and nanoparticles. *J. Mater. Chem.* **2005**, *15*, 3745−3760.

(4) Sacanna, S.; Pine, D. J.; Yi, G. -R Engineering shape: The novel geometries of colloidal self-assembly. *Soft Matter* **2013**, *9*, 8096−8106.

(5) Li, F.; Josephson, D. P.; Stein, A. Colloidal assembly: The road from particles to colloidal molecules and crystals. *Angew. Chem., Int. Ed.* **2011**, *50*, 360−388.

(6) Van Blaaderen, A. Materials science: Colloids get complex. *Nature* **2006**, *439*, 545−546.

(7) Jana, N. R.; Gearheart, L.; Murphy, C. J. Seeding growth for size control of 5−40 nm diameter gold nanoparticles. *Langmuir* **2001**, *17*, 6782−6786.

(8) Tao, A.; Sinsermsuksakul, P.; Yang, P. Polyhedral silver nanocrystals with distinct scattering signatures. *Angew. Chem., Int. Ed.* **2006**, *45*, 4597−4601.

(9) Shchepelina, O.; Kozlovskaya, V.; Singamaneni, S.; Kharlampieva, E.; Tsukruk, V. V. Replication of anisotropic dispersed particulates and complex continuous templates. *J. Mater. Chem.* **2010**, *20*, 6587−6603.

(10) Lekkerkerker, H. N. W.; Vroege, G. J. Liquid crystal phase transitions in suspensions of mineral colloids: new life from old roots. *Philos. Trans. R. Soc., A* **2013**, *371*, 20120263.

(11) Thies-Weesie, D. M. E.; De Hoog, J. P.; Hernandez Mendiola, M. H.; Petukhov, A. V.; Vroege, G. J. Synthesis of goethite as a model colloid for mineral liquid crystals. *Chem. Mater.* **2007**, *19*, 5538−5546.

(12) Krehula, S.; Popović, S.; Musić, S. Synthesis of acicular α-FeOOH particles at a very high pH. *Mater. Lett.* **2002**, *54*, 108−113.

(13) Ye, X.; Jin, L.; Caglayan, H.; Chen, J.; Xing, G.; Zheng, C.; Doan-Nguyen, V.; Kang, Y.; Engheta, N.; Kagan, C. R.; Murray, C. B. Improved size-tunable synthesis of monodisperse gold nanorods through the use of aromatic additives. *ACS Nano* **2012**, *6*, 2804−2817.

(14) Ebbesen, T. W.; Ajayan, P. M. Large-scale synthesis of carbon nanotubes. *Nature* **1992**, *358*, 220−222.

(15) Carbone, L.; Nobile, C.; De Giorgi, M.; Della Sala, F.; Morello, G.; Pompa, P.; Hytch, M.; Snoeck, E.; Fiore, A.; Franchini, I. R.; Nadasan, M.; Silvestre, A. F.; Chiodo, L.; Kudera, S.; Cingolani, R.; Krahne, R.; Manna, L. Synthesis and micrometer-scale assembly of colloidal CdSe/CdS nanorods prepared by a seeded growth approach. *Nano Lett.* **2007**, *7*, 2942−2950.

(16) Wagner, R. S.; Ellis, W. C. Vapor-liquid-solid mechanism of single crystal growth. *Appl. Phys. Lett.* **1964**, *4*, 89−90.

(17) Mokari, T.; Rothenberg, E.; Popov, I.; Costi, R.; Banin, U. Selective growth of metal tips onto semiconductor quantum rods and tetrapods. *Science* **2004**, *304*, 1787−1790.

(18) Halpert, J. E.; Porter, V. J.; Zimmer, J. P.; Bawendi, M. G. Synthesis of CdSe/CdTe nanobarbells. *J. Am. Chem. Soc.* **2006**, *128*, 12590−12591.

(19) Sacanna, S.; Pine, D. J. Shape-anisotropic colloids: Building blocks for complex assemblies. *Curr. Opin. Colloid Interface Sci.* **2011**, *16*, 96−105.

(20) Rossi, L.; Sacanna, S.; Irvine, W. T. M.; Chaikin, P. M.; Pine, D. J.; Philipse, A. P. Cubic crystals from cubic colloids. *Soft Matter* **2011**, *7*, 4139−4142.

(21) Sugimoto, T.; Khan, M. M.; Muramatsu, A. Preparation of monodisperse peanut-type α-Fe_2O_3 particles from condensed ferric hydroxide gel. *Colloids Surf., A* **1993**, *70*, 167−169.

(22) Park, J. -W; Park, Y. J.; Jun, C. -H Post-grafting of silica surfaces with pre-functionalized organosilanes: New synthetic equivalents of conventional trialkoxysilanes. *Chem. Commun.* **2011**, *47*, 4860−4871.

(23) Kuijk, A.; Van Blaaderen, A.; Imhof, A. Synthesis of monodisperse, rodlike silica colloids with tunable aspect ratio. *J. Am. Chem. Soc.* **2011**, *133*, 2346−2349.

(24) Zhang, J.; Liu, H.; Wang, Z.; Ming, N. Au-induced polyvinylpyrrolidone aggregates with bound water for the highly shape-selective synthesis of silica nanostructure. *Chem. - Eur. J.* **2008**, *14*, 4374−4380.

(25) Kuijk, A.; Byelov, D. V.; Petukhov, A. V.; Van Blaaderen, A.; Imhof, A. Phase behavior of colloidal silica rods. *Faraday Discuss.* **2012**, *159*, 181−199.

(26) Kuijk, A.; Troppenz, T.; Filion, L.; Imhof, A.; Van Roij, R.; Dijkstra, M.; Van Blaaderen, A. Effect of external electric fields on the phase behavior of colloidal silica rods. *Soft Matter* **2014**, *10*, 6249−6255.

(27) He, J.; Yu, B.; Hourwitz, M. J.; Liu, Y.; Perez, M. T.; Yang, J.; Nie, Z. Wet-Chemical Synthesis of Amphiphilic Rodlike Silica Particles and their Molecular Mimetic Assembly in Selective Solvents. *Angew. Chem., Int. Ed.* **2012**, *51*, 3628−3633.

(28) Morgan, A. R.; Dawson, A. B.; Mckenzie, H. S.; Skelhon, T. S.; Beanland, R.; Franks, H. P. W.; Bon, S. A. F. Chemotaxis of catalytic silica-manganese oxide "matchstick" particles. *Mater. Horiz.* **2014**, *1*, 65−68.

(29) Longbottom, B. W.; Rochford, L. A.; Beanland, R.; Bon, S. A. F. Mechanistic Insight into the Synthesis of Silica-Based "matchstick" Colloids. *Langmuir* **2015**, *31*, 9017−9025.

(30) Zhang, A. -Q; Li, H. -J; Qian, D. -J; Chen, M. Kinetically-controlled template-free synthesis of hollow silica micro-/nanostructures with unusual morphologies. *Nanotechnology* **2014**, *25*, 135608.

(31) Datskos, P.; Sharma, J. Synthesis of segmented silica rods by regulation of the growth temperature. *Angew. Chem., Int. Ed.* **2014**, *53*, 451−454.

(32) Datskos, P.; Chen, J.; Sharma, J. Addressable morphology control of silica structures by manipulating the reagent addition time. *RSC Adv.* **2014**, *4*, 2291−2294.

(33) Kuijk, A.; Imhof, A.; Verkuijlen, M. H. W.; Besseling, T. H.; van Eck, E. R. H.; Van Blaaderen, A. Colloidal silica rods: Material properties and fluorescent labeling. *Particle and Particle Systems Characterization* **2014**, *31*, 706−713.

(34) Van Blaaderen, A.; Vrij, A. Synthesis and characterization of colloidal dispersions of fluorescent, monodisperse silica spheres. *Langmuir* **1992**, *8*, 2921−2931.

(35) Hell, S. W.; Wichmann, J. Breaking the diffraction resolution limit by stimulated emission: stimulated-emission-depletion fluorescence microscopy. *Opt. Lett.* **1994**, *19*, 780−782.

(36) Hell, S. W. Far-field optical nanoscopy. *Science* **2007**, *316*, 1153−1158.

(37) Willig, K. I.; Harke, B.; Medda, R.; Hell, S. W. STED microscopy with continuous wave beams. *Nat. Methods* **2007**, *4*, 915−918.

(38) Van Blaaderen, A.; Van Geest, J.; Vrij, A. Monodisperse colloidal silica spheres from tetraalkoxysilanes: Particle formation and growth mechanism. *J. Colloid Interface Sci.* **1992**, *154*, 481−501.

(39) Iler, R. K. *The Chemistry of Silica: Solubility, Polymerization, Colloid and Surface Properties and Biochemistry of Silica*; Wiley: New York, 1979.

(40) Brinker, C. J.; Sehgal, R.; Hietala, S. L.; Deshpande, R.; Smith, D. M.; Loy, D.; Ashley, C. S. Sol-gel strategies for controlled porosity inorganic materials. *J. Membr. Sci.* **1994**, *94*, 85−102.

(41) Wong, Y. J.; Zhu, L.; Teo, W. S.; Tan, Y. W.; Yang, Y.; Wang, C.; Chen, H. Revisiting the Stöber method: Inhomogeneity in silica shells. *J. Am. Chem. Soc.* **2011**, *133*, 11422−11425.

(42) van der Voort, H. T. M.; Strasters, K. C. Restoration of confocal images for quantitative image analysis. *J. Microsc.* **1995**, *178*, 165−181.

DOI: 10.1021/acs.langmuir.6b00678
Langmuir 2016, 32, 3970−3976